



## Eikonal Approximation for $K^+$ -Nucleus Elastic Scattering

Nagat A. ELMAHDY<sup>1\*</sup>, Haytham GAMAL<sup>2</sup>

<sup>1</sup> Basic Science Department, Modern Academy for Engineering and Technology, Cairo, Egypt  
\* Corresponding Author Email : [nagat\\_elmahdy@yahoo.com](mailto:nagat_elmahdy@yahoo.com) ORCID: 0000-0002-6152-5842

<sup>2</sup> Electronics Engin. and Communication Technology Dep. Modern Academy for Engin. and Technology, Cairo, Egypt  
Email : [haytham\\_gamal8@hotmail.com](mailto:haytham_gamal8@hotmail.com) ORCID: 0000-0003-0880-2011

### Article Info:

DOI: 10.22399/ijcesen.1079685  
Received : 27 February 2022  
Accepted : 14 April 2022

### Keywords

Equivalent local potential  
Eikonal approximation  
Kaon elastic scattering cross section  
Scattering amplitudes parameters  
Nuclear density distributions

### Abstract:

The elastic scattering of kaons from different targets  ${}^6\text{Li}$ ,  ${}^{12}\text{C}$ , and  ${}^{40}\text{Ca}$  at energies 635, 715, and 800 MeV have been studied. The equivalent local potential form of Kisslinger optical potential with the eikonal approximation using Wallace expansion up to the 2<sup>nd</sup> order have been used. The potential depends on the density of the target nuclei, and the scattering amplitude parameters. Satisfactory fits to the elastic scattering experimental data are obtained.

## 1. Introduction

It is known that the  $K^+$  meson scattering can be used as a weak hadronic interacting probe for investigating the neutron density distributions in nuclei which is providing insights into the nature of the scattering. Therefore the experimental data on elastic differential cross sections at intermediate energies [1,2] are under the permanent attention of theoreticians for years. Many optical model analyses of the elastic scattering of kaons from nuclei have been carried out using potentials of the Kisslinger form [3], its local equivalent form is introduced by Johnson [4], microscopic optical potential [5], and other forms for different nuclear density models.

The first and second-order corrections to the zero order eikonal phase shifts for heavy-ion elastic scattering based on the Coulomb trajectories of colliding nuclei have been applied satisfactory and improve the agreement with the experimental data [6]. Also this work extended to cover the charged pions scattering on nuclei by using the Coulomb modified eikonal phase shift and its first order correction [7]. It has been applied satisfactory to 800 MeV/c pions scattering from  ${}^{12}\text{C}$  and  ${}^{40}\text{Ca}$

nuclei. The overall results are in excellent agreement at momentum 800 MeV/c and the agreement extended to the angle  $36^\circ$ . The local form of the Kisslinger optical potential succeeded before with the eikonal approximation model in analysis of pion scattering without recourse to the complexities of the nonlocal interactions [8,9].

Among all the hadronic probes,  $K^+$  meson holds special properties, below 1 GeV/c, the  $K^+$ -N strong interaction has a slow energy and momentum dependence and it is the weakest of all strong-interaction processes [10].

Because of the quark content of the  $K^+$  which can't annihilate with valence quark content of the nucleon,  $K^+$  has a long mean free path in the nuclear matter and capable of probing the interior of nuclei. A small cross section means a long mean free path ( $\lambda = \frac{1}{\rho\sigma} > 5fm$ ) for propagation of the  $K^+$  in the nuclear medium, in contrast to the strongly interacting particles which get absorbed at the surface [11], so it is an ideal probe to study nuclear structure, and for a light nucleus, such as  ${}^{12}\text{C}$ , the uncertainties which appear in working with the strong interaction are much smaller [12].

Recently, Ebrahim [10] proposed that the equivalent local optical potential with the zero-range distorted-wave Born approximation can be used to analyze the  $K^+$ -nucleus elastic scattering but needs an enhancement in the dominated S11  $K^+$ -N phase shift by 10 % for  ${}^6\text{Li}$  and around 12 % for  ${}^{12}\text{C}$ , and  ${}^{40}\text{Ca}$  nuclei. The DWUCK4 code is used to calculate the angular distributions with distorted-wave Born approximation. The charge distribution is used for  ${}^6\text{Li}$ , the harmonic oscillator form for  ${}^2\text{H}$  and  ${}^{12}\text{C}$ , and the three parameter Fermi 3PF shape distribution of nucleons is used for  ${}^{40}\text{Ca}$ .

The Ericson-Ericson Lorentz-Lorentz (EELL) parameter  $\zeta$  slightly affects the elastic scattering. The disagreement between the calculated results and data at  $K^+$ - ${}^{12}\text{C}$  is about 15% at 800 MeV/c but appears to decrease with decreasing momenta [10]. A good agreement by using the 3PF distribution density for the  ${}^{40}\text{Ca}$  at 800 MeV/c and the polarization  $\zeta = 1.0$  is obtained by increasing the S11 phase shift by 12%. If the  $K^+$ -N phase shifts increase the nucleon size will increase; a ‘‘swelling’’ of the nucleon in the nuclear medium. This means that the  $K^+$ -N interaction inside a nucleus will differ from the free space. The local optical potential can serve as a reliable model for kaon-nucleus scattering.

Lukyanov [5] used the derived microscopic optical potential in calculation of the differential elastic-scattering cross sections for the interaction of  $K^+$  mesons with  ${}^{12}\text{C}$  and  ${}^{40}\text{Ca}$  nuclei at energies 635, 715, and 800 MeV. It is determined by the amplitude for kaon–nucleon scattering and the density distribution of point like nucleons of the target nucleus. The results obtained by calculating optical potentials depend on the density distributions of point like neutrons and protons in the ground state of the nucleus. It turns out that, in this model, there is no need for including nonlocal terms in the potential, in contrast to what is done in the Kisslinger model, or for employing phenomenological optical-model potentials involving a large number of free parameters.

Originally, the eikonal approximation has taken a considerable attention after the work of Glauber [13] who obtained a Fourier-Bessel representation of the scattering amplitude which justified for all angles on general grounds of analyticity in the momentum transfer. Glauber extended it by using a frozen target approximation to convert the many body scattering problem into a potential scattering problem in which the potential depends on the coordinates of the target. Wallace [14] proposed a sequence of four approximations to the exact

impact parameter of the scatterin matrix. In eikonal propagation picture, the accelerated projectile propagates through a frozen target without changing its transverse position but picking up an eikonal phase [15].

The present study of the  $K^+$  scattering is focused on eikonal approximation with its first and second corrections. This interest has been particularly motivated by a hope to explain well the  $K^+$ -nucleus elastic scattering data. We give a simple physical description to the quantum mechanical formulation of the eikonal propagation which has been extensively used in hadronic interaction problems in dense (nuclear) environment at high energy. This is illustrated that by calculating the differential cross sections with the first and second order eikonal corrections [15]. For the first time the local potential of Johnson and Satchler [4], together with the eikonal approximation with 2<sup>nd</sup> order corrections were used to analyze the angular distributions of elastically scattered  $K^+$  from  ${}^6\text{Li}$ ,  ${}^{12}\text{C}$ , and  ${}^{40}\text{Ca}$  at kaon lab momenta ranging from 635-800 MeV/c. Satisfactory agreement with the measured angular distributions and the local optical potential calculation is obtained at forward angles. MATLAB CODE is used for all calculations and formulas. The present work is precisely an attempt to understand the range of validity and limits of the applicability of the eikonal approximation by using local Kisslinger optical potential. In Sec.II the basic formulas of the potential equations and an explicit quantum mechanical description of the eikonal approximation are given. Sec. III is devoted to the results and discussions followed by conclusion in Sec. IV.

## 2. Formalism

Meson-nucleus elastic scattering data are analyzed using an optical potential of the Kisslinger form [3]. By using the Krell-Ericson transformation [16] and solving of the Klein-Gordon equation. The basic equation of the phenomenological local optical potential will be

$$U(r) = \frac{(\hbar c)^2}{2\omega} \left( \frac{q(r)}{1-\alpha(r)} - \frac{k^2\alpha(r)}{1-\alpha(r)} - \left( \frac{\frac{1}{2}\nabla^2\alpha(r)}{1-\alpha(r)} + \left( \frac{\frac{1}{2}\nabla\alpha(r)}{1-\alpha(r)} \right)^2 \right) \right) + \frac{\alpha(r)V_c - \left( \frac{V_c^2}{2\omega} \right)}{1-\alpha(r)} \quad (1)$$

which introduced as potential without sharp edge. The quantities  $q(r)$  and  $\alpha(r)$  can be expressed in terms of meson-nucleon scattering amplitudes and the target nucleus density distributions with their

gradients. The quantities  $q(r)$  and  $\alpha(r)$  are complex quantities depend on energy and target densities (proton and neutron densities). They defined as fellows

$$q(r) = q_0(r) + \Delta q(r) \quad (2)$$

$$\alpha(r) = \frac{\alpha_1(r)}{1 + \frac{1}{3}\zeta\alpha_1(r)} + \alpha_2(r) \quad (3)$$

$$\text{where, } q_0(r) = -4\pi p_1(b_0\rho(r) - b_1\Delta\rho(r)) \quad (4)$$

$$\Delta q(r) = -\frac{1}{2}\varepsilon\nabla^2\left(\alpha_1(r) + \frac{1}{2}\alpha_2(r)\right) \quad (5)$$

$$\alpha_1 = 4\pi\frac{(c_p\rho(r) - c_1\Delta\rho(r))}{1 + (\omega/Mc^2)} \quad (6)$$

$$\alpha_2 = 4\pi\frac{(c_p\rho_{np}(r) - c_1\rho(r)\Delta\rho(r))}{1 + (\omega/2Mc^2)} \quad (7)$$

and

$$\rho(r) = \rho_n(r) + \rho_p(r) \quad (8)$$

$$\Delta\rho(r) = \rho_n(r) - \rho_p(r) \quad (9)$$

$$\rho_{np}(r) = 4\rho_n(r)\rho_p(r) \quad (10)$$

where  $\rho_p(r)$  and  $\rho_n(r)$  are proton and neutron density distributions of target nucleus, respectively. We use  $p_1$  and  $p_2$  as kinematic constants which depend on meson energy.  $M$  is the mass of a nucleon and  $\omega$  is the total energy of meson in the centre of mass [17].  $\zeta$  is the Ericson-Ericson Lorentz-Lorentz (EELL) parameter which parameterizes the polarization of the nuclear medium [18]. The  $\zeta$  parameter isn't exactly known because its determination requires taking into account all the effects together which make the calculation unreliable [19]. This parameter has a small effect above the  $\Delta$ -resonance in the calculations compared to its effect in the resonance energy. The quantities  $b_i$  and  $c_i$  ( $i = 0,1$ ) are referred to the first order amplitude parameters, while the complex amplitude second-order parameters  $B_i$  and  $C_i$  ( $i = 0,1$ ) describe the pion absorption. Different formulas of the radial density distribution for the considered nuclei are used. The formulas are the charge distribution density (CH), the harmonic oscillator (HO) model, the two parameter Fermi (2PF) model, and the three parameter Fermi (3PF) model, all are used to clarify the general changes in the radial variations of the density from one nucleus to another. CH density model gives information about the charge density and hence primarily about the proton distribution and it takes the form [10]

$$\rho_{ch}(r) = \frac{Z}{8\pi^{3/2}}\left[\frac{1}{a^3}\exp\left(\frac{-r^2}{4a^2}\right) - \frac{c^2(6b^2 - r^2)}{4b^7}\exp\left(\frac{-r^2}{4b^2}\right)\right] \quad (11)$$

where  $a$ , and  $b$  are adjustable parameters,  $Z$  is the atomic number and extended to be taken for neutron density form, its domain of use for light nuclei and it will be named CH model. The Harmonic Oscillator (HO) is defined as [4]:

$$\rho(r) = \rho_0\left[1 + \alpha\left(\frac{r}{c}\right)^2\right]\exp\left[-\left(\frac{r}{c}\right)^2\right] \quad (12)$$

where  $c$  is a parameter related to root mean square radius,  $\alpha$  is the oscillator constant and  $\rho_0$  is the density of nuclear matter at  $r = 0$ . The two-parameter Fermi (2PF) is defined as [4]:

$$\rho_i(r) = \frac{\rho_{oi}}{1 + \exp\left(\frac{r - c_i}{a_i}\right)} \quad (13)$$

where  $i = n$  or  $p$  for proton or neutron, and  $c$  is the half density radius,  $a$  is the diffuseness parameter (a measure of the thickness of the surface layer of nucleus) and  $\rho_0$  is the central density parameter.

The three-parameter Fermi (3PF) is defined as [18]:

$$\rho_i(r) = \frac{\rho_{oi}\left(1 + \frac{\omega_i r^2}{c_i^2}\right)}{1 + \exp\left(\frac{r - c_i}{a_i}\right)} \quad (14)$$

where  $i = n$  or  $p$  for proton or neutron respectively, and  $c_i$  is the half density radius,  $a_i$  is the diffuseness,  $\rho_0$  is the central density parameter and  $\omega_i$  is an adjustable parameter. All the density forms of neutrons and protons are subjected to the normalization condition:

$$\int \rho_i(\bar{r}) d\bar{r} = (A - Z) \text{ or } Z \quad (15)$$

where  $Z$  is the atomic number of the nucleus and in particular it leads for 3PF and 2PF density models. The nuclear density is taken as

$$\rho(r) = \rho_n(r) + \rho_p(r) \quad (16)$$

All the parameters of these three types of densities are listed in Table 1 and 2.

**Table 1:** The ground-state density distributions parameters and the densities of nuclear matter for the charged density, the harmonic oscillator, 2PF, and 3PF models ( $p$  for protons).

Nucleus	Model	$c_p$	$a_p$	$w_p$	$\rho_{0p}$	Ref
<sup>6</sup> Li	3PF	1.55	0.07	0.015	0.08	*
	2PF	2.063	0.096	0	0.08	*
<sup>12</sup> C	3PF	2.002	0.5	0.2595	0.08	[20]
	2PF	2.5	0.37	0	0.075	[21]
<sup>40</sup> Ca	3PF	3.68	0.546	-0.1	0.0743	[22]
	2PF	3.42	0.55	0	0.0951	[22]
Nucleus	Model	$a$	$b$ and $\alpha$	$C$	$\rho_{0p}$	Ref
<sup>6</sup> Li	CH	0.928	1.26	0.48	0.51262	[10]
	HO	1.727	4.5		0.08994	*
<sup>12</sup> C	CH	0.928	1.26	0.48	0.1538	*
	HO	1.516	2.234		0.0711	[10]
<sup>40</sup> Ca	CH	0.928	1.26	0.48	0.51262	*
	HO	1.727	4.5		0.08994	*

\* The values stated in all tables are satisfying the root mean square radius for each nucleus.

**Table 2:** The ground-state density distributions parameters and the densities of nuclear matter for the charged density, the harmonic oscillator, 2PF, and 3PF models ( $n$  for protons).

Nucleus	Model	$c_n$	$a_n$	$w_n$	$\rho_{0n}$	Ref
${}^6\text{Li}$	3PF	1.55	0.07	0.015	0.08	*
	2PF	2.063	$\frac{0.09}{6}$	0	0.08	*
${}^{12}\text{C}$	3PF	2.002	0.5	0.2595	0.08	[20]
	2PF	2.5	0.37	0	0.075	[21]
${}^{40}\text{Ca}$	3PF	3.97	0.42	-0.1	0.0743	[22]
	2PF	3.42	0.55	0	0.0951	[22]
Nucleus	Model				$\rho_{0n}$	Ref
${}^6\text{Li}$	CH				0.51262	[10]
	HO				0.08994	*
${}^{12}\text{C}$	CH				0.15380	*
	HO				0.0711	[10]
${}^{40}\text{Ca}$	CH				0.51262	*
	HO				0.08994	*

\* The values stated in all tables are satisfying the root mean square radius for each nucleus.

According to Wallace, the expansion of the phase shift function  $\chi(b)$ , as a power series in the strength of the scattering potential and its derivatives [6]

$$\chi_i(b) = \sum_{n=0}^j \chi^{(n)}(b) \quad (18)$$

where

$$\chi^{(n)}(b) = -\frac{k[\mu/(\hbar k)^2]}{(n+1)! b^{2n}} \left[ b^2 \left( 1 + b \frac{d}{db} \right) \right]^n \int_0^\infty U^{n+1} [(b^2 + z^2)^{1/2}] dz \quad (19)$$

The zero order term in Eqn. (19) gives the eikonal phase shift

$$\chi^{(0)}(b) = -\frac{\mu}{\hbar^2 k} \int_0^\infty U \left( (b^2 + z^2)^{\frac{1}{2}} \right) dz \quad (20)$$

For local potential the first and second order corrections are given, respectively, by

$$\chi^{(1)}(b) = -\frac{\mu^2}{2\hbar^4 k^3} \left( 1 + b \frac{d}{db} \right) \int_0^\infty U^2 \left( (b^2 + z^2)^{\frac{1}{2}} \right) dz \quad (21)$$

$$\chi^{(2)}(b) = -\frac{\mu^3}{6\hbar^6 k^5} \left( 3 + 5b \frac{d}{db} + b^2 \frac{d^2}{db^2} \right) \int_0^\infty U^3 \left( (b^2 + z^2)^{\frac{1}{2}} \right) dz \quad (22)$$

where  $U$  is the optical potential,  $b$  is the impact parameter,  $\mu$  is the reduced mass, and  $k$  is momentum in the centre of mass system. The  $S$  matrix is expressed as

$$S_l = \exp(2i\delta_l), \quad \text{and} \quad \delta_l = \frac{1}{2} \chi(b) \quad (23)$$

The general expression for the elastic scattering amplitude between the spin 0 kaon and the target nucleus is given by

$$f(\theta) = f_c(\theta) + (2ik)^{-1} \sum_l (2l+1) \exp(2i\eta_l) (S_l - 1) P_l(\cos \theta) \quad (24)$$

where  $f_c(\theta)$  is the Coulomb scattering amplitude,  $k$  is the centre of mass momentum, and  $\eta_l$  is the Coulomb phase shift [23]. The differential cross section is given by

$$\frac{d\sigma}{d\Omega} = |f(\theta, \Omega)|^2 \quad (25)$$

### 3. Results and Discussion

#### A. The Eikonal Phase Shift with Wallace corrections

The eikonal phase shifts with Wallace corrections up to 2<sup>nd</sup> order have been used to calculate the elastic scattering differential cross section of  $K^+$ -nucleus as shown in figures (1-3). All these calculations have been done for  $\zeta = 1$  (the polarization parameter). Fig. 1 shows with the reaction  $K^+ - {}^6\text{Li}$  at energy 715 MeV using 2PF nuclear density model. Fig. 2 shows with the reaction  $K^+ - {}^{12}\text{C}$  at a) energy 635 MeV using CH nuclear density model, b) at energy 715 MeV using HO model for the target density. From what proceeds, it can be seen that calculation with different corrections up to 2<sup>nd</sup> order of the eikonal expansion has no effect on the calculated elastic scattering differential cross section. The Figures 1-2 show no effect of higher order corrections on the results of the elastic cross section, since the relatively small kaon mass to its momentum ratio, converges the eikonal expansion rapidly. The eikonal phase shift corrected up to second order term is calculated using the same scattering amplitude parameters of Ebrahim [24,25]. Figures 3 shows the calculations of the elastic scattering differential cross section of  $K^+$ -nucleus depending on these parameters for the reactions  $K^+ + {}^6\text{Li}$  at energy 715 MeV, and  $K^+ + {}^{12}\text{C}$  at energy 635 MeV. It presents that the result doesn't agree well with the experimental data although it comes close for lower target masses and incident energies. The

eikonal model didn't come very well with these taken amplitude parameters [24,25]. Such approach with previously used scattering amplitude parameters didn't fit properly the data and eventually get a limited success. In the case of the eikonal approach, since the parameters of the scattering amplitudes are based on the free kaon-nucleon scattering. This keeping structural frame of the scattering amplitudes to get the best possible values to fit different targets and energies with different models of nuclear densities to obtain the best possible fit with the eikonal approach for scattering. The resulting best fit scattering amplitude parameters used in the present work for  $K^\pm$  nucleus are shown in Tables 3, 4, and 5. The difference in the two approximations, the partial wave impulse approximation, in which the binding forces are ignored during collision, and the eikonal approximations sticks to the straight line path as a

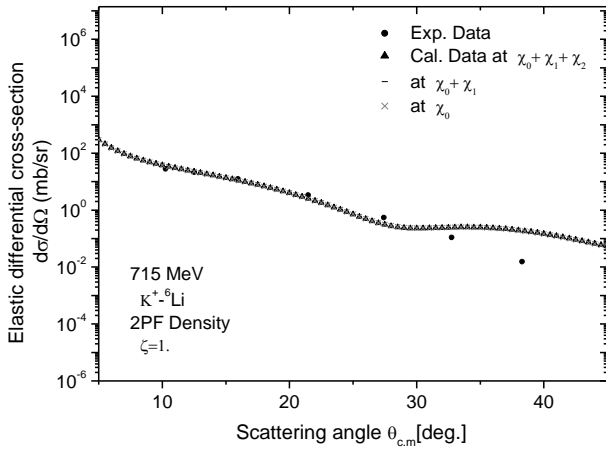


**Figure 1.** The elastic scattering cross sections for  $K^+ + {}^6\text{Li}$  with 2PF density model by using the zero, first and the second-order terms of the eikonal phase shifts at 715 MeV. The experimental data is taken from Ref.[26].

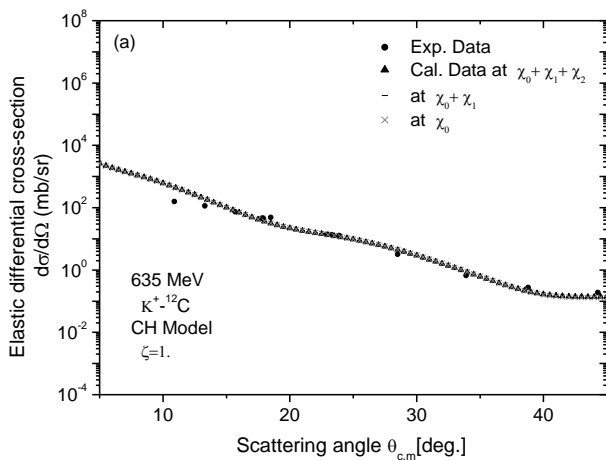


**Figure 2.** The elastic scattering cross sections for  $K^+ + {}^{12}\text{C}$  using the zero, first and the second-order terms of the eikonal phase shifts (a) CH model at 635 MeV, (b) HO model at 715 MeV. The experimental data is taken from Ref.[26].

**Table 3:** First-order amplitude parameters used in the present work with  $K^+$  as a projectile and ( ${}^6\text{Li}$ ,  ${}^{40}\text{Ca}$ ) as targets. Note: in each case the upper row is the real part and the lower row is the imaginary part for each target.

	${}^6\text{Li}$	${}^{40}\text{Ca}$
$T_\pi$ (MeV)	715	800
$k$ ( $\text{fm}^{-1}$ )	4.66	5.86
$p_1$	2.11	2.34
$p_2$	1.56	1.67
$b_0$ (fm)	0.07892	2.0165
	0.034847	1.121890
$b_1$ (fm)	0.03622	0.03567
	0.1155600	0.0353200
$c_0$ ( $\text{fm}^3$ )	0.005949	-0.05047
	0.1153390	0.090000
$c_1$ ( $\text{fm}^3$ )	0.01502	0.01352
	-0.0447327	0.0143100

**Table 4:** First-order amplitude parameters used in the present work with  $K^+$  as a projectile and  ${}^{12}\text{C}$  as target. Note: in each case the upper row is the real part and the lower row is the imaginary part for each target.

	${}^{12}\text{C}$	${}^{12}\text{C}$	${}^{12}\text{C}$
$T_\pi$ (MeV)	635	715	800
$k$ ( $\text{fm}^{-1}$ )	4.688	5.066	5.456
$p_1$	2.12	2.2	2.26
$p_2$	1.56	1.6	1.63
$b_0$ (fm)	2.232501	2.3658	2.116427
	1.021470	2.648000	-0.167816
$b_1$ (fm)	0.026355	-0.0593	0.033963
	-0.041603	0.0536000	0.0648988
$c_0$ ( $\text{fm}^3$ )	-0.09629	0.00212	-0.051
	0.1937890	0.1673000	0.3724900
$c_1$ ( $\text{fm}^3$ )	-0.03406	0.006173	-0.01464
	-0.0144586	-0.0491000	0.0008428

**Table 5:** Second-order amplitude parameters used in the present work with  $K^+$  as a projectile. Note: in each case the upper row is the real part and the lower row is the imaginary part for each target.

	${}^6\text{Li}$	${}^{12}\text{C}$	${}^{12}\text{C}$	${}^{12}\text{C}$	${}^{40}\text{Ca}$
$T_\pi$ (MeV)	715	635	715	800	800
$C_0$ ( $\text{fm}^3$ )	0	0	0	-2.8	-3.6
	0	0	0	-3.6	1.0
$C_1$ ( $\text{fm}^3$ )	0	0	0	0	0
	0	0	0	0	0

special direction which makes a stringent semiclassical limit. These conceptual differences reflect on the different values of the amplitude parameters for fitting the experimental data at each method. So, with eikonal model, it is possible to get the agreement with data only with the variation of the amplitude parameters freely and isn't possible to get it with previously calculated parameters. This makes the problem more complicated and pushes the way to find The difference in the two approximations, the partial wave impulse approximation, in which the binding forces are ignored during collision, and the eikonal approximations sticks to the straight line path as a

special direction which makes a stringent semiclassical limit. These conceptual differences reflect on the different values of the amplitude parameters for fitting the experimental data at each method. So, with eikonal model, it is possible to get the agreement with data only with the variation of the amplitude parameters freely and isn't possible to get it with previously calculated parameters. This makes the problem more complicated and pushes the way to find a more systematic way to the correlation between the scattering amplitudes calculated before and those obtained at best possible fit.

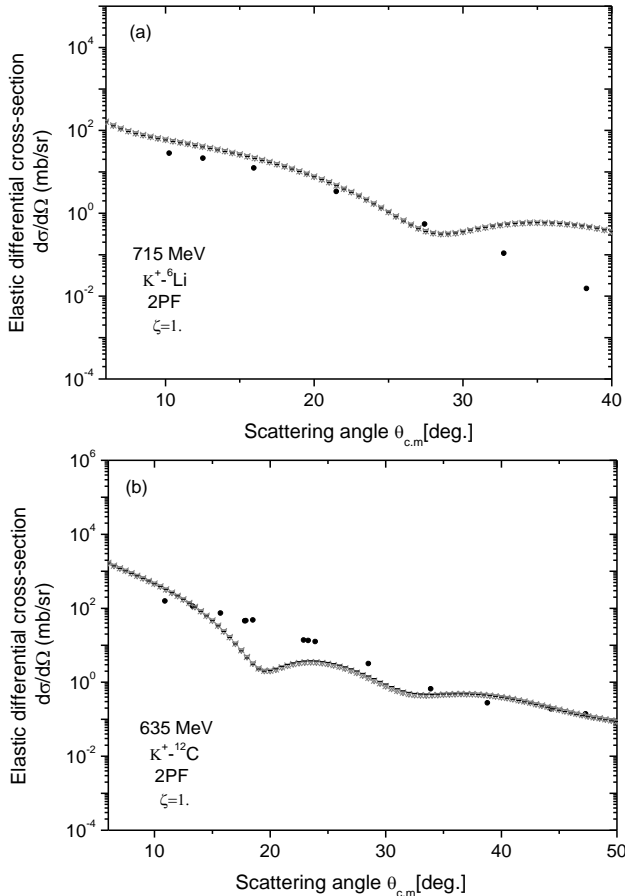


**Figure 3.** The elastic scattering cross sections (a) for  $K^+ + {}^6\text{Li}$  with 2PF density model at 715, (b) for  $K^+ + {}^{12}\text{C}$  with 2PF density model at 635 MeV. The scattering amplitude parameters are from Ref.[24,25]. The experimental data is taken from Ref.[26].

### B. Effect of the target density model

The local potential terms depend on the target nuclear density distribution. To study this factor, four different models of the nuclear densities which describe the shape of the target nucleus, all are used to clarify the general changes in the radial variations of the density from one nucleus to another. The values of  $\zeta = 1$ , has been used in all calculations. The fitted scattering amplitude

parameters of Table 2 have been used in all the following calculations of the elastic scattering differential cross section of  $K^+$ -nucleus.

$K^+ + {}^6\text{Li}$ : Figures (4-5) show our calculation of  $K^+ + {}^6\text{Li}$  using different types of target density model (CH, HO, 2PF, 3PF) compared with experimental data.

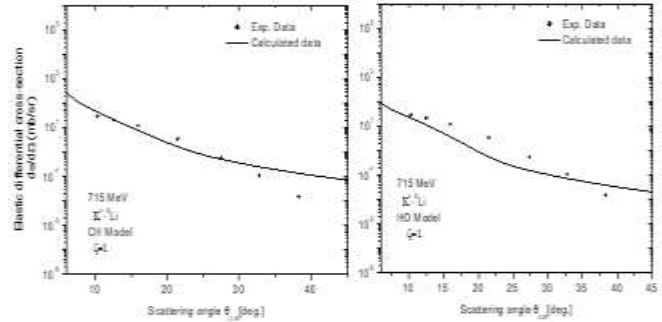


**Figure 4.** The elastic scattering of  $K^+ + {}^6\text{Li}$  by using CH and HO density model with  $\zeta=1$  at energy 715 MeV. The experimental data is taken from Ref.[26].

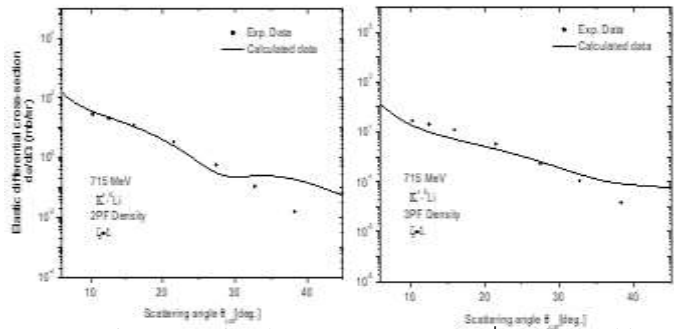


**Figure 5.** The elastic scattering of  $K^+ + {}^6\text{Li}$  and by using 2PF and 3PF density model with  $\zeta=1$  at energy 715 MeV. The experimental data is taken from Ref.[26].

Clearly, the best fitting obtained among the target's densities is the 2PF model with the eikonal approach. The core density plays an important part at large scattering angles.

$K^+ + {}^{12}\text{C}$ : Similarly, by applying calculation of  $K^+ + {}^{12}\text{C}$  using different types of target density model (CH, HO, 2PF, 3PF), it is found the 2PF and 3PF models of density have limited agreement and produce a minimum moves to smaller angles with increasing the energy. The best fitting obtained among the target's densities is the CH model with the eikonal approach as shown in Figure (6).

$K^+ + {}^{40}\text{Ca}$ : Figure (7) shows our calculation of  $K^+ + {}^{40}\text{Ca}$  using different types of target density model (2PF, 3PF) compared with the experimental data. The 2PF and 3PF distributions are shown for  ${}^{40}\text{Ca}$ . These two models have been only used because the

CH and HO failed to describe the heavier nuclei. It could be seen that the calculations with the 2PF model for the density of the target nucleus  $^{40}\text{Ca}$  gives the best results at small angles as shown in figures. The following Table 6 shows all the best density models with each target and energy, which summaries the present work results of  $\text{K}^+$  with  $^6\text{Li}$ ,  $^{12}\text{C}$ , and  $^{40}\text{Ca}$

**Table 6:** the scattering angle range of agreement for the elastic differential cross sections of  $\text{K}^+$  with different targets with their best density model at different energies.

Projectile	Energy (MeV)	Target	Best Density Model	Agreement Range
$\text{K}^+$	715	$^6\text{Li}$	2PF	$10^\circ$ to $33^\circ$
	635	$^{12}\text{C}$	CH	$10^\circ$ to $50^\circ$
	715	$^{12}\text{C}$	CH	$10^\circ$ to $40^\circ$
	800	$^{12}\text{C}$	HO	$10^\circ$ to $30^\circ$
	800	$^{40}\text{Ca}$	2PF	$10^\circ$ to $15^\circ$

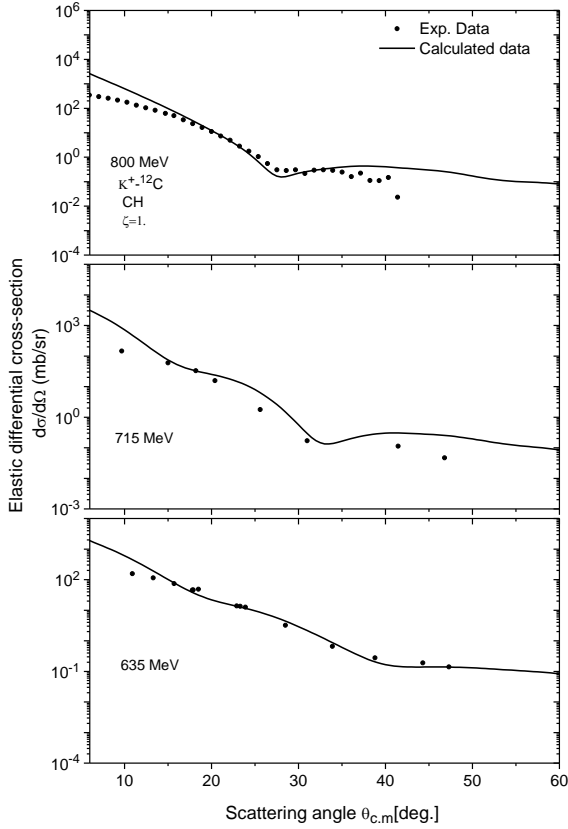


**Figure 6.** The elastic scattering of  $\text{K}^+ + ^{12}\text{C}$  by using CH density model with  $\zeta=1$  at energies; 635 MeV, 715 MeV, and 800 MeV. The experimental data is taken from Ref.[26,27].

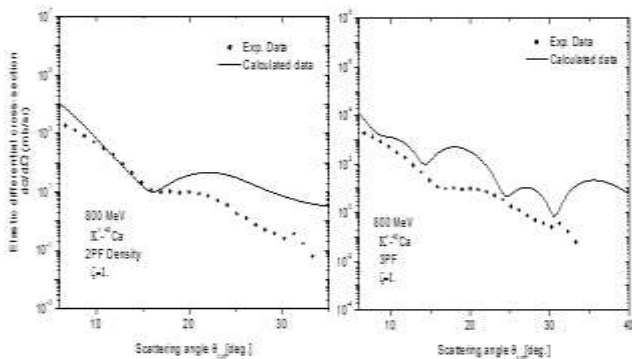


**Figure 7.** The elastic scattering of  $\text{K}^+ + ^{40}\text{Ca}$  by using 2PF and 3PF density model with  $\zeta=1$  at energy 800 MeV. The experimental data is taken from Ref.[26].

#### 4. Conclusion

We have studied the angular distributions of the elastic scattering differential cross sections for  $\text{K}^+$  on  $^6\text{Li}$ ,  $^{12}\text{C}$ , and  $^{40}\text{Ca}$  at energies 635, 715, and 800 MeV. Where we show how well the eikonal approximation model and local form of Kisslinger were able to reproduce the experimental data. To this purpose we have used the eikonal model by considering the first and the second-order correction terms to the eikonal phase shifts. Also, the local Kisslinger optical potential depends on different sets of free adjustable parameters; the type of density model, the amplitude parameters, and the EELL parameters. It seems clear that a full analysis of these parameters will be required if a detailed comparison is to be made with the experimental results. The accuracy of the agreement with experimental data can be improved by changing these parameters to reach the best fit.

The higher order corrections would clarify the relationship between the eikonal expansion and the impact parameter  $b$ . Corrections, which are incorporated to the eikonal expansion, have nearly no effect on the results because of the massive projectile and its large momentum. The correlation parameter  $\zeta$  parameterizes the polarization of the nuclear medium.

The availability of change the EELL parameter gave nearly no change on the calculated elastic scattering cross sections in the experimental range of angles. In order to check for possible density-dependent effects, the four sets of density models are applied. For the nuclear density distributions, it was assumed that the proton and neutron densities were similar. From the comparison with the experimental data, the 2PF model of density gives satisfactory results with the most cases of interactions. The CH model of nuclear density predictions was suitable with  $^{12}\text{C}$  and the 2PF nuclear density model predicted well the calculated results for  $^6\text{Li}$  and  $^{40}\text{Ca}$ . 3PF model was the worst in most cases of study.

In deriving the amplitudes parameters, it is necessary to transform the kaon-nucleon scattering amplitude from the two-body centre of mass system to the kaon-nucleus centre of mass system. The most significant difference between the free nucleon cases and fitted parameters are that the fitted magnitude of  $\text{Re}(b_0)$ ,  $\text{Im}(b_0)$ ,  $\text{Re}(c_0)$ , and  $\text{Im}(c_0)$ . In addition, adding values for the second-order amplitudes parameters  $\text{Re}(C_0)$  contributes to give the best fitting. The present elastic scattering data can be well reproduced by local form of Kisslinger potential with adjustable parameters which rather different than the free kaon-nucleon values. We note that the regularization of the local Kisslinger optical potential used in this work by the introduction of the fitting parameters can serve as a tool to obtain a best agreement with the experimental data.

After having made an adjustment of the potential parameters, and using the suitable model of density, we have deduced a set of potential parameters which describe the elastic scattering cross sections for nuclei under examination. It is found also that the effective potential parameters slightly change from nucleus to nucleus.

The local Kisslinger model with the eikonal model was found to be successful for all types of interactions in the present work. The close agreement between theory and experiment is mainly for the forward angles less than  $40^\circ$  and in fair agreement with  $40^\circ < \theta < 50^\circ$ . As a whole the eikonal model description is quite successful as a framework for a description of  $K^+$ - nucleus scattering. In addition to being a study of the eikonal model, this work also provided a systematic and comprehensive local Kisslinger potential model analysis of mesons-nucleus scattering. The calculated cross sections reproduced the experimental data quite well for the considered nuclei.

### Author Statements:

- **Ethical approval:** The conducted research is not related to either human or animal use.
- **Conflict of interest:** The authors declare that they have no known competing financial interests or personal relationships that could have appeared to influence the work reported in this paper
- **Acknowledgement:** The authors declare that they have nobody or no-company to acknowledge.

- **Author contributions:** The authors declare that they have equal right on this paper.
- **Funding information:** The authors declare that there is no funding to be acknowledged.
- **Data availability statement:** The data that support the findings of this study are available on request from the corresponding author. The data are not publicly available due to privacy or ethical restrictions.

### References

- [1] D. Marlow, P. D. Barnes, N. J. Colella, S. A. Dytman, R. A. Eisenstein, R. Grace, F. Takeutchi, W. R. Wharton, S. Bart, D. Hancock, R. Hackenberg, E. Hungerford, W. Mayes, L. Pinsky, T. Williams, R. Chrien, H. Palevsky, and R. Sutter (1982) Kaon scattering from C and Ca at 800 MeV/c". *Phys. Rev. C* 25: 2619.
- [2] R.E.Chrien, R.Sawafta, R.J.Peterson, R.A.Michael, and E.V.Hungerford. (1997) Elastic and Inelastic Scattering of  $K^+$  from  ${}^6\text{Li}$  and  ${}^{12}\text{C}$ . *Nucl. Phys. A* 625: 251. DOI: 10.1016/S0375-9474(97)00384-9
- [3] L. S. Kisslinger. (1955) Scattering of Mesons by Light Nuclei *Phys. Rev.* 98:761. DOI:https://doi.org/10.1103/PhysRev.98.761
- [4] M. B. Johnson and G. R. Satchler. (1996) Characteristics of local pion-nucleus potentials that are equivalent to Kisslinger-type potentials. *Ann. Phys., NY* 248:134.
- [5] V. K. Lukyanov, E. V. Zemlyanaya, K. V. Lukyanov, D. N. Kadrev, A. N. Antonov, M. K. Gaidarov, and S. E. Massen(2009) Calculations of  $8\text{He}+p$  Elastic Cross Sections Using Microscopic Optical Potential. *Arxiv*: 0908.1008 V1 [nucl. th].
- [6] Moon Hoe Cha, and Yong Joo Kim. (1995) Higher-order corrections to the eikonal phase shifts for heavy-ion elastic collision. *Phys. Rev. C* 5:212-216. DOI:https://doi.org/10.1103/PhysRevC.51.212
- [7] Moon Hoe Cha, and Yong Joo Kim. (1996) First-order eikonal approximation for the elastic scattering of 800 MeV/c pions from  ${}^{12}\text{C}$  and  ${}^{40}\text{Ca}$  nuclei *Phys. Rev. C* 54:429. DOI: 10.1103/PhysRevC.54.429
- [8] M. B. Johnson (1980) Analytical theory of pion single and double charge exchange in resonance region. I. Geometrical limit. *Phys. Rev. C* 22:192. DOI:https://doi.org/10.1103/PhysRevC.22.192
- [9] M. B. Johnson and E. R. Siciliano. (1983) Isospin dependence of second order pion nucleus optical potential. *Phys. Rev. C* 27:730-750. DOI:https://doi.org/10.1103/PhysRevC.27.730
- [10] A. A. Ebrahim and S. A. E. Khallaf. (2002) Elastic and inelastic scattering of  $K^+$  from nuclei *Phys. Rev. C* 66:044614. DOI: https://doi.org/10.1103/PhysRevC.66.044614
- [11] R. Weiss, J. Aclander, J. Alster, M. Barakat, S. Bart, R. E. Chrien, R.A. Krauss, K. Johnston, L Mardor, Y. Mardor, S. May Tal-beck, E. Piasetzky, P. H. Pile, R. Sawafta, H. Seyfarth, R. L. Stearns, R.J.



- Sutter and A.I. Yavin. (1994) Measurement of low energy  $K^+$  total cross sections on  $N=Z$  nuclei *Phys. Rev. C* 49: 2569.
- [12] R. Micheal, M. Barakat, S. Bart, R. E. Chrien, D. J. Ernest, S. Hama, K. H. Hicks, Wendy Hinton, E. V. Hungerford, M. F. Jiang, T. Kishimoto, C. M. Kormanyos, L. J. Kurth, L. Lee, B. Mayes, R. J. Peterson, L. Pinsky, R. Sawafta, R. Sutter, L. Tang, and J. E. Wise. (1996)  $K^+$  elastic scattering from C and Li-6 at 715-MeV/c. *Phys. Lett. B* 382:29-34.
- [13] R. J. Glauber. (1959) High-Energy Collision Theory, edited by W. E. Britten Interscience, *New York*.
- [14] S. J. Wallace. (1973) Eikonal expansion” *Ann. of Phys.* 78:190-257. DOI: [https://doi.org/10.1016/0003-4916\(73\)90008-0](https://doi.org/10.1016/0003-4916(73)90008-0)
- [15] Alex Kover, and Urs Achim Weidemann. (2001) Eikonal evolution and gluon radiation. *Phys. Rev. D* 64:114002.
- [16] M. Krell and T. E. O. Ericson (1969) Energy levels and wave functions of pionic atoms. *Nucl. Phys. B* 11:521-550. DOI: [https://doi.org/10.1016/0550-3213\(69\)90301-0](https://doi.org/10.1016/0550-3213(69)90301-0)
- [17] Reza Safari. (2006) A new pion-nucleus optical potential valid for  $\Delta$ -resonance region. *International Journal of Pure and Applied Mathematics.* 29(2):141-151.
- [18] S.A.E. Khallaf and A.A. Ebrahim. (2000) Analysis of  $\pi^\pm$ -nucleus elastic scattering using a local potential. *Phys. Rev. C* 62:024603. DOI:<https://doi.org/10.1103/PhysRevC.62.024603>
- [19] Ricardo Ignacio Alvarez del Castillo, (1991) Ph.D. Thesis, *McGill University Montreal, Canada*,
- [20] R. Alvarez del Castillo and N. B. de Takacsy (1991) Analysis of low energy  $\pi^+$  scattering to second  $O^+$  states. *Phys. Rev. C* 43:1389. DOI:<https://doi.org/10.1103/PhysRevC.43.1389>
- [21] B. M. Preedom, S. H. Dam, C. W. Darden, III, R. D. Edge, D. J. Malbrough, T. Marks, R. L. Burman, M. Hamm, M. A. Moinester, R. P. Redwine, M. A. Yates, F. E. Bertrand, T. P. Cleary, E. E. Gross, N. W. Hill, C. A. Ludemann, M. Blecher, K. Gotow, D. Jenkins, and F. Milder. (1981) Positive pion-nucleus elastic scattering at 30 and 50 MeV. *Phys. Rev. C* 23:1134. DOI: 10.1103/PhysRevC.23.1134
- [22] K. G. Boyer, W. J. Braithwaite, W. B. Cottingham, S. J. Greene, L. E. Smith, C. Fred Moore, C. L. Morris, H. A. Thiessen, G. S. Blanpied, G. R. Burleson, J. F. Davis, J. S. McCarthy, R. C. Minehart, and C. A. Goulding (1984) Pion elastic and inelastic scattering from  $^{40,42,44,48}\text{Ca}$  and  $^{54}\text{Fe}$ . *Phys. Rev. C* 29:182. DOI: <https://doi.org/10.1103/PhysRevC.29.182>
- [23] M. Y. M. Hassan, Z. Metawei (2002) First and second order corrections to the eikonal phase shifts for the interactions of  $\alpha$ -particle with  $^{12}\text{C}$  and  $\text{Ca}$  isotopes. *Acta Physica Slovaca.* 52: 23-34.
- [24] A.A. Ebrahim and R.J. Peterson (1996) Parametrization of pion-nucleon phase shifts and effects upon pion-nucleus scattering calculations. *Phys. Rev. C* 54: 2499. DOI: <https://doi.org/10.1103/PhysRevC.54.2499>
- [25] A. A. Ebrahim, (1997) Ph.D. Thesis, Assiut University.
- [26] R. E. Chrien, R. Sawafta, R. J. Peterson, R. A. Michael, and E. V. Hungerford (1997) Elastic and Inelastic Scattering of  $K^+$  from  $^6\text{Li}$  and  $^{12}\text{C}$ . *Nucl. Phys. A* 625:251. DOI: [https://doi.org/10.1016/S0375-9474\(97\)00384-9](https://doi.org/10.1016/S0375-9474(97)00384-9)
- [27] D. Marlow, P. D. Barnes, N. J. Colella, S. A. Dytman, R. A. Eisenstein, R. Grace, F. Takeutchi, W. R. Wharton, S. Bart, D. Hancock, R. Hackenberg, E. Hungerford, W. Mayes, L. Pinsky, T. Williams, R. Chrein, H. Palevsky, and R. Sutter . (1982) Kaon Scattering from C and Ca at 800 MeV/c. *Phys. Rev. C* 25: 2619.